Available online at www.sciencedirect.com
SCIENCE DIRECT®
Chemical Physics Letters 414 (2005) 384–388
CHEMICAL PHYSICS LETTERS
www.elsevier.com/locate/cplett

The *Liesegang eyes* phenomenon

Mátyás Ripszám [a], Ádám Nagy [a], András Volford [b], Ferenc Izsák [c,d], István Lagzi [a,*]

[a] *Department of Physical Chemistry, Eötvös University, P.O. Box 32, Budapest H-1518, Hungary*
[b] *Department of Chemical Physics, Budapest University of Technology and Economics, Budapest H-1521, Hungary*
[c] *Department of Applied Analysis, Eötvös University, P.O. Box 120, Budapest H-1518, Hungary*
[d] *Department of Applied Mathematics, University of Twente, P.O. Box 217, 750 AE Enschede, The Netherlands*

Received 12 July 2005
Available online 13 September 2005

Abstract

Radially symmetric pattern formation phenomena were investigated experimentally and numerically in 2D using a new experimental arrangement in a precipitation system. We examined the dependence of the pattern structure and the evolution of the precipitation front on its curvature. Depending on the radius of the reaction medium, two types of precipitation patterns has been observed: (a) pattern with a continuously distributed precipitate and a well detectable precipitation-free domain (*Liesegang eyes* phenomenon); (b) pattern with a continuous precipitation zone and discrete ring formation. Results of our simulations are in a good agreement with the experimental observations.

1. Introduction

Classical Liesegang patterns are produced in the wake of a moving reaction front [1]. These structures are well-known examples of spatiotemporal selforganization. In the simplest situation, an electrolyte, called outer electrolyte, diffuses into a reaction medium (in the experiments, it is usually a gel) and reacts with another electrolyte (inner electrolyte) that is uniformly distributed in this medium. The precipitation reaction between them produces an insoluble precipitate product, which is usually distributed quasiperiodically in the gelled medium. Studies on the above phenomena are of great importance, since complex patterns observed in chemical [2], biological [3,4] and geochemical [5] systems can be described in the similar manner.

The presence of precipitation bands or rings is related to the geometry of the experimental setup [6–15]. Basic geometrical arrangement of the experiments can be divided into two categories: planar and circular (spherical) boundary conditions can be applied. In the first case (this is the usual approach), one electrolyte is placed into a test tube within a gel matrix, while the outer electrolyte is placed on top of the gel column. Here, the precipitation bands (1D) or parallel zones (2D, 3D) are expected to be perpendicular to the diffusion front of the invading (outer) electrolyte. In case of the 2D (or even 3D) radial geometrical setup, the inner electrolyte is placed in a gelled medium in a Petri dish and a solution of the outer electrolyte is added into its center. The reaction front will move from the center to the periphery of the dish producing separated precipitation rings behind. Empirical regularities (time – [16], spacing – [17,18], width – [19,20], and Matalon–Packter law [21–23]) describing the evolution and the final pattern structure, have been considered in case of a planar motion of the reaction fronts. The propagation velocity of the chemical waves is highly depending on their curvature (curvature effect); this has been studied for the chemical (BZ) waves in details [24]. This effect plays also an important role in the signal processing in an excitable medium [25,26] and in the stability of the chemical flame balls [27]. Although Liesegang patterning is a heterogeneous process and in this respect it

* Corresponding author. Fax: +36 13722 592.
E-mail addresses: ripszam@vuk.chem.elte.hu (M. Ripszám), xadam@para.chem.elte.hu (Á. Nagy), volfi@phyndi.fke.bme.hu (A. Volford), izsakf@cs.elte.hu (F. Izsák), lagzi@vuk.chem.elte.hu (I. Lagzi).

0009-2614/$ - see front matter © 2005 Elsevier B.V. All rights reserved.
doi:10.1016/j.cplett.2005.08.093

differs substantially from the excitable systems, it is interesting and important to analyze the effect of the front curvature on the pattern structure.

The aim of the present Letter is to investigate the evolution of the Liesegang pattern using a new radial geometrical setup. In this concept, we have performed the experiments in a completely new arrangement. The inner electrolyte is placed in a gel disk of a small width and the outer electrolyte diffuses from outside into a gel disk producing various types of precipitation patterns. Numerical simulations based on pre-nucleation theory were also performed to explain our experimental results [28].

2. Experimental

An agarose gel disk swollen by 0.05 M KI solution with thickness of 1.8 mm was prepared as follows. 0.40 g of agarose (Reanal) was dissolved in 40 ml of distillated water. The solution was heated to 80–90 °C and stirred until the solution became crystal clear (approx. 5 min). The solution was then poured into a Petri dish, which was hold firmly horizontal to obtain a uniformly thick gel. After the completion of the gelation (approx. 15 min) the gel disks were cut at different radii (4, 5, 6, 7 and 8 mm) and put into a 0.05 M KI (inner electrolyte) solution for 30 min.

One side of the disk was slightly smeared with silicon grease and glued in this way to the bottom of the Petri dish. This will also avoid the penetration of the outer solution into the gel from this bottom side. The experiment was started by pouring 0.5 M $Pb(NO_3)_2$ (outer electrolyte) solution around the gel, and taking extreme care not to allow the solution to flow over the gel. As a result of this, the outer solution can penetrate into the gel only from sideward.

The pattern formation was monitored in transmitted light from a neon lamp by a CCD camera (Panasonic WV-CP410) connected to a computer. The pictures were taken in every 30 s until the pattern evolution is completed.

3. Model and simulation

A simple (AB-type) precipitation process can be described by the following chemical equation:

$$\mathrm{A(aq)} + \mathrm{B(aq)} \rightarrow \mathrm{P(s)}, \tag{1}$$

where P(s) denotes the precipitate. In case of a radially symmetric experimental arrangement, the governing reaction-diffusion equations are the following:

$$\frac{\partial a}{\partial \tau} = D_a \frac{\partial^2 a}{\partial r^2} + D_a \frac{N-1}{r}\frac{\partial a}{\partial r} - \delta(ab, K, L), \tag{2a}$$

$$\frac{\partial b}{\partial \tau} = D_b \frac{\partial^2 b}{\partial r^2} + D_b \frac{N-1}{r}\frac{\partial b}{\partial r} - \delta(ab, K, L), \tag{2b}$$

$$\frac{\partial p}{\partial \tau} = \delta(ab, K, L) \tag{2c}$$

for $0 < \tau < \tau_{\max}$ and $0 < r < R_0$. Here, $a(\tau,r)$ and $b(\tau,r)$ denote the concentrations, D_a and D_b are the diffusion coefficients of the species A(aq) and B(aq) associated to the outer and the inner electrolytes, respectively, while $p(\tau,r)$ is the amount of the precipitate. In our description, all these quantities were dimensionless. $\delta(ab,K,L)$ is called the precipitation reaction term, based on Ostwald's supersaturation theory [28]. The spatial variable r gives the distance from the center, while τ is the time variable and N gives the number of spatial dimensions. The second term on the right hand side of the Eqs. (2a) and (2b) describes the effect of curvature on the diffusion.

The precipitation reaction term $\delta(ab,K,L)$ is defined as follows [29,30] :

$$\delta(ab, K, L) = \begin{cases} \kappa\delta_{\mathrm{p}}\Theta(ab - K) & \text{if } p = 0, \\ \kappa\delta_{\mathrm{p}}\Theta(ab - L) & \text{if } p > 0, \end{cases} \tag{3}$$

where κ is the rate constant of the precipitation reaction (1), K is the nucleation product, L is the solubility product, and Θ yields the Heaviside step function. δ_{p} is increment of the reaction product, and is calculated from equation $(a - \delta_{\mathrm{p}})(b - \delta_{\mathrm{p}}) = L$. The basic idea of the model is that precipitation occurs only if the product of the concentrations reaches the nucleation product (K). At the same time, if previously formed precipitate is present, it promotes the precipitation process, therefore, in this case the product of the concentrations has to reach only a lower threshold (precipitation product L). Precipitate formation was limited in the simulations, if $p > p_{\max}$, the precipitation process was stopped.

System (2a)–(2c) has been solved numerically using a "method of lines" technique. We can convert (2a)–(2c) into a set of ordinary differential equations after spatial discretization (finite difference) on an equidistant 1D spatial grid. The produced ordinary differential equations have been integrated in time using a second order Runge–Kutta method while the system (2a)–(2c) has been equipped with the following boundary conditions:

$$a|_{r=R_0} = a_0 \quad \text{and} \quad \left.\frac{\partial a}{\partial r}\right|_{r=0} = \left.\frac{\partial b}{\partial r}\right|_{r=0} = \left.\frac{\partial b}{\partial r}\right|_{r=R_0} = 0$$
$$\text{for} \quad 0 < \tau < \tau_{\max},$$

where a_0 is the initial concentration of the outer electrolyte and R_0 is the radius of the reaction medium (gel disk), respectively. This ensures a uniform flux of the invading electrolyte from outside and the no-flux boundary condition for the inner electrolyte ensures that it is distributed into the gel during the reaction. The following setup of concentrations has been chosen as initial conditions:

$$a(0,r) = 0, \; b(0,r) = b_0 \quad \text{and} \quad p(0,r) = 0$$
$$\text{for} \quad 0 < r < R_0,$$

where b_0 is the initial concentration of the inner electrolyte. Initially, B(aq) is the only species in the reaction medium. Most of the parameters in (2a)–(2c) were kept constant as follows: $D_a = D_b = 0.4$, $K = 0.11$, $L = 0.1$, $\kappa = 10^3$ and $p_{\max} = 5.0$. The grid spacing and the time step were $\Delta r = 0.4$ and $\Delta\tau = 0.001$, respectively.

4. Results and discussion

Fig. 1 shows the precipitate distributions governed by curvature of the reaction fronts for two radii of the gel disk. Two different types of patterns can be observed depending on the radius of the reaction medium. In case of smaller radii, a continuous precipitation front evolves. Increasing the radius, additionally, a family of rings develops. Nevertheless, in all cases the center of the gel disk does not contain precipitate, because the fast precipitation process (compared to the diffusion) depletes the inner electrolyte in the vicinity of the front. Accordingly, by and by the inner electrolyte fully reacts in the reaction medium. Therefore, the front stops and leaves in the center of the gel disk a strict and well visible precipitation-free domain. We call the formation of such patterns the *Liesegang eyes* phenomenon.

Now, we will focus on the evolution of the PbI_2 pattern in the experiments. The most trivial regularity from the existing laws is the time law, which describes that the position of the nth band (measured from the junction point of the electrolytes) is linearly proportional to the square root of time elapsed until its formation, i.e., $X_n \propto t_n^{1/2}$ [16,18]. This law applies to all geometries where the reaction front is closely planar. We have monitored the evolution of the precipitation front instead of ring formation, because the formation of distinct zones is absent for smaller radii. The precipitation density distribution has been determined by an image processing system. The evolution curve showing the position of the precipitation front versus the square root of time is displayed in Fig. 2. According to the generally accepted time law, the above curve is linear as long as the front is planar. In our case, however, the fronts are circular, and velocity of the precipitation front propagation (vs. square root of time) is accelerated due to the curvature effect. During the evolution, the curvature of the front is increased, which results in higher and higher diffusion flux. It should be noted that despite of the increased mass flux of the invading electrolyte, the pattern formation is stopped if the precipitation process depletes the inner electrolyte in the gel disk.

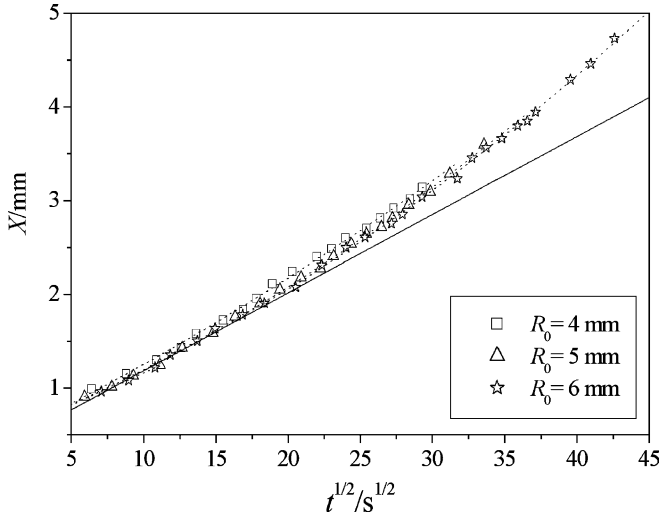

Fig. 2. Experimental evolution of the precipitation fronts for different radii of the gel disk (reaction medium). The dotted lines are the fitted second-order curves. The solid line represents the linear curve fitted for the first five points for $R_0 = 6$ mm.

In case of continuous precipitation, the relative size of the precipitation-free hole has a regularity, if we pose the following assumptions:

(a) the investigated system is *two*-dimensional and satisfies the mass conservation law;
(b) all species of the inner electrolyte B(aq) transform into precipitate (the non-reacted part is negligible to the initial one);
(c) the density of the precipitate ($\bar{p}$) is constant behind the reaction front and does not depend on the curvature.

Using (a)–(c), we obtain the following relation:

$$(R_0^2 - r_0^2)\pi\bar{p} = R_0^2\pi b_0,$$

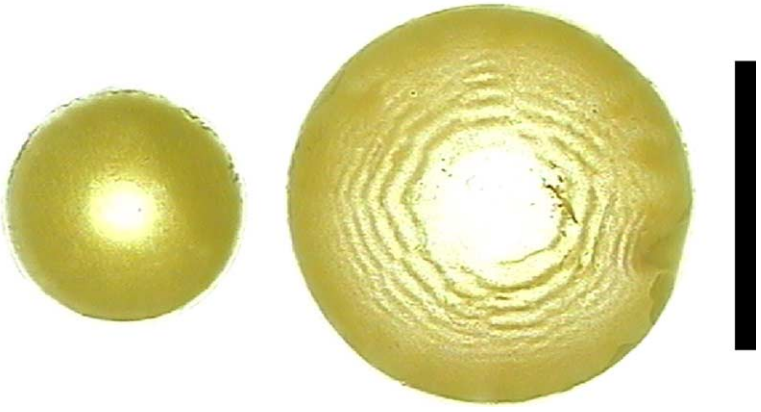

Fig. 1. The two-dimensional precipitation patterns of lead iodine in agarose gel at 22.0± 1.0 °C: $R_0 = 4$ mm (left) and $R_0 = 7$ mm (right). The scale bar is 1 cm.

where b_0 is initial concentration of the inner electrolyte, R_0 and r_0 are the radius of the reaction medium and precipitation-free domain, respectively. We can rewrite the equation above as

$$\frac{r_0^2}{R_0^2} = \frac{\bar{p} - b_0}{\bar{p}}, \tag{4}$$

which states that the quotient of the radius of the precipitation-free and the reaction domain should be constant, if all parameters of the system except of the domain radius (R_0) are fixed. Our investigation cleared that continuous precipitation zone formation is preferred at smaller temperature. Therefore, these experiments were performed at 8.8 ± 0.2 °C. The validation of our predictions is shown in Table 1. The quotient of the corresponding radii can be considered constant within an experimental error. This simple consideration makes possible to estimate the average density of the precipitate ($\bar{p}$) behind the reaction front, because in the relation (4) b_0 is known, while r_0 and R_0 are measurable in the experiments.

Table 1
Dependence of r_0^2/R_0^2 on radius of the reaction domain

R_0	5 mm	6 mm	7 mm	8 mm
r_0^2/R_0^2	4.27×10^{-2}	5.29×10^{-2}	5.26×10^{-2}	5.63×10^{-2}

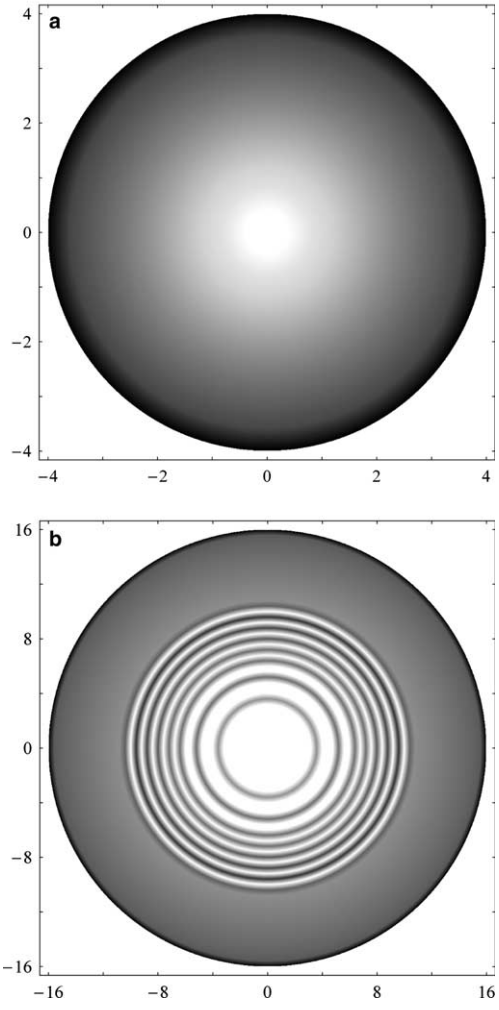

Fig. 3. Results of the numerical simulations: the two-dimensional precipitation patterns at $R_0 = 4$ (a) and $R_0 = 16$ (b).

Compared with the experimental results, numerical simulations exhibit a similar trend with respect to the radius dependent pattern structure and its evolution. Fig. 3 presents the 2D precipitate distribution for two different domains. The time law in a 1D setup states that the position of the precipitate bands vs. the square root of their appearance time is linear. In the radial 2D case, however, the diffusion term in (2a)–(2c) consists of two part, where the second one $\frac{N-1}{r}$, associated to the curvature effect, is

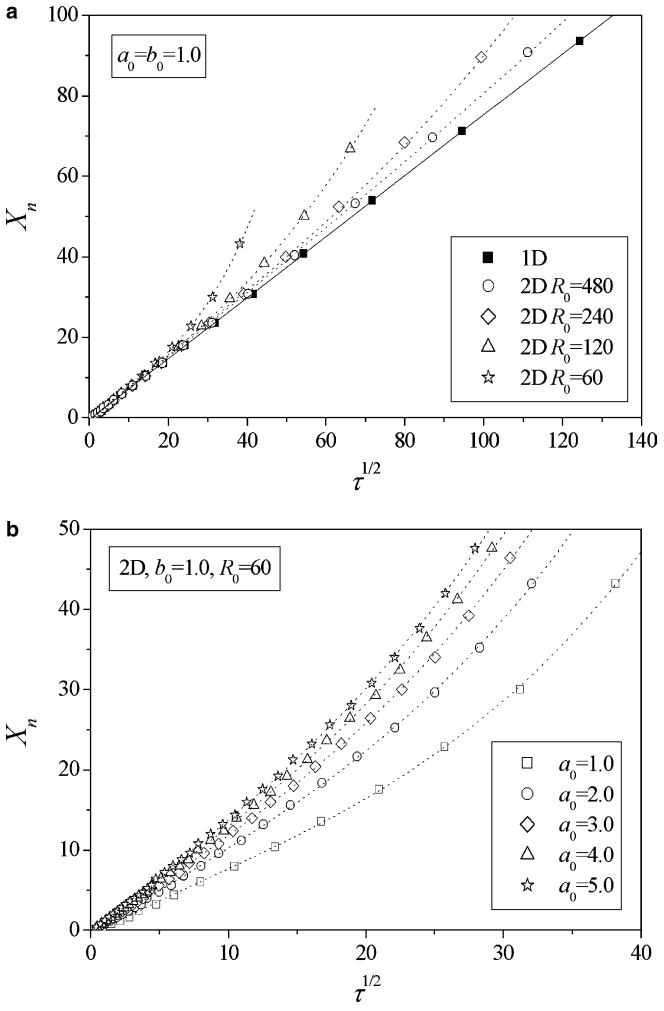

Fig. 4. Simulated evolution of the precipitation patterns for different radii of the reaction medium (a) fixed the initial concentration of both electrolytes and simulated evolution of the precipitation patterns for different initial concentration of the outer electrolyte (b) fixed the initial concentration of the inner electrolyte and the radius of the reaction medium. The dotted lines represent the fitted (a) second- and (b) third-order polynomials, while the solid line is the fitted linear curve in a 1D simulation. X_n is the position of the nth precipitation band measured from the junction point of the electrolytes, while τ is the appropriate formation time.

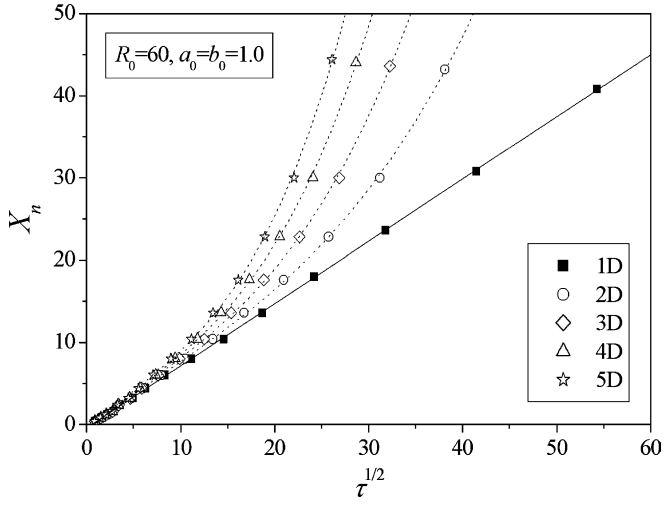

Fig. 5. Simulated evolution of the precipitation patterns for different spatial dimensions by fixed initial concentration of the electrolytes and the radius of the reaction medium. The dotted lines are the fitted third-order curves. The solid line represents the fitted linear curve in 1D simulation. X_n is the position of the nth precipitation band measured from the junction point of the electrolytes, while τ is the appropriate formation time.

usually not negligible. The decrease of R_0 generates a more and more pronounced deviation from the linear time law (Fig. 4a). This distortion can be described very accurately by a second-order function, according to the experiments. We have also investigated the effect of the outer electrolyte concentration on the evolution of the precipitation pattern for fixed R_0 (Fig. 4b). Increasing the concentration results in an accelerated evolution and approximates a linear dynamics. By increasing the spatial dimension (N), the second term in 2a and 2b, associated to the curvature effect, becomes more significant, which can recognized as a faster front propagation (Fig. 5).

In conclusion, we reported the important role of the curvature effect for the pattern structure and evolution in precipitation systems. Experiments were performed using a new two-dimensional experimental setup with radial arrangements by varying the radius of the reaction medium. Numerical simulations were carried out with the appropriate initial and boundary conditions in two and three dimensions. Moreover, we proceed in higher dimensions: this theoretical study helped us to point out the effect of the curvature on the evolution dynamics. The curvature effect and final pattern structures found in the model calculations and in the experiments have shown a good agreement. In addition, we provided a new simple method to estimate the average amount of the precipitate behind the front using only geometrical measurements.

Acknowledgements

The authors thank Prof. Zoltán Noszticzius for his contribution to the experimental work. We acknowledge the support of the Hungarian OTKA Grant T042708 and OTKA Postdoctoral Fellowship (Grant Number D048673).

References

[1] R.E. Liesegang, Naturwiss. Wochenschr. 11 (1896) 353.
[2] S.C. Müller, J. Ross, J. Phys. Chem. A 107 (2003) 7997.
[3] V.V. Kravchenko, A.B. Medvinskii, V.I. Emelyanenko, A.N. Reshetilov, G.R. Ivanitskii, Biofizika 45 (2000) 93.
[4] A.B. Medvinskii, A.V. Rusakov, M.A. Tsyganov, V.V. Kravchenko, Biofizika 45 (2000) 525.
[5] T. Geisler, A.M. Seydoux-Guillaume, M. Wiedenbeck, R. Wirth, J. Berndt, M. Zhang, B. Mihailova, A. Putnis, E.K.H. Salje, J. Schluter, Am. Mineral. 89 (2004) 1341.
[6] H.-J. Krug, H. Brandtstädter, J. Phys. Chem. A 103 (1999) 7811.
[7] R. Sultan, S. Panjarian, Physica D 157 (2001) 241.
[8] I. Das, S. Chand, A. Pushkarna, J. Phys. Chem. 93 (1989) 7435.
[9] I. Das, A. Pushkarna, A. Bhattacharjee, J. Phys. Chem. 95 (1991) 3866.
[10] L. Zeiri, O. Younes, S. Efrima, M. Deutsch, Phys. Rev. Lett. 79 (1997) 4685.
[11] U. Sydow, P.J. Plath, Ber. Bunsenges. Phys. Chem. 102 (1998) 1683.
[12] F. Arteaga-Larios, E.Y. Sheu, E. Perez, Energ. Fuel. 18 (2004) 1324.
[13] I. Lagzi, A. Volford, A. Büki, Chem. Phys. Lett. 396 (2004) 97.
[14] M. Fialkowski, A. Bitner, B.A. Grzybowski, Phys. Rev. Lett. 94 (2005) 018303.
[15] E.L. Cabarcos, C.S. Kuo, A. Scala, R. Bansil, Phys. Rev. Lett. 77 (1996) 2834.
[16] H.W. Morse, G.W. Pierce, Proc. Am. Acad. Arts. Sci. 38 (1903) 625.
[17] K. Jablczynski, Bull. Soc. Chim. Fr. 33 (1923) 1592.
[18] J. George, G. Varghese, Chem. Phys. Lett. 362 (2002) 8.
[19] K.M. Pillai, V.K. Vaidyan, M.A. Ittyachan, Colloid Polym. Sci. 258 (1980) 831.
[20] M. Droz, J. Magnin, M. Zrínyi, J. Chem. Phys. 110 (1999) 9618.
[21] R. Matalon, A. Packter, J. Colloid. Sci. 10 (1955) 46.
[22] T. Antal, M. Droz, J. Magnin, Z. Rácz, M. Zrínyi, J. Chem. Phys. 109 (1998) 9479.
[23] J. George, I. Paul, P.A. Varughese, G. Varghese, Pramana. J. Phys. 60 (2003) 1259.
[24] J.J. Tyson, J.P. Keener, Physica D 32 (1988) 327.
[25] Á. Tóth, V. Gáspár, K. Showalter, J. Chem. Phys. 98 (1994) 522.
[26] J. Sielewiesiuk, J. Gorecki, J. Phys. Chem. A 106 (2002) 4068.
[27] É. Jakab, D. Horváth, J.H. Merkin, S.K. Scott, P.L. Simon, Á. Tóth, Phys. Rev. E 66 (2002) 016207.
[28] W. Ostwald, Kolloid Z. 36 (1925) 380.
[29] A. Büki, É. Kárpáti-Smidróczki, M. Zrínyi, J. Chem. Phys. 103 (1995) 10387.
[30] A. Büki, É. Kárpáti-Smidróczki, M. Zrínyi, Physica A 375 (1995) 357.